

# First-principles studies on the intrinsic stability of the magic $\text{Fe}_{13}\text{O}_8$ cluster

Q. Sun and Q. Wang

*Institute for Materials Research, Tohoku University, Sendai 980-8577, Japan*

K. Parlinski

*Institute for Materials Research, Tohoku University, Sendai 980-8577, Japan  
and Institute of Nuclear Physics, 31-342 Cracow, Poland*

J. Z. Yu

*Institute for Materials Research, Tohoku University, Sendai 980-8577, Japan*

Y. Hashi

*Hitachi Tohoku Software Ltd., Sendai 980-0014, Japan*

X. G. Gong

*Institute of Solid State Physics, Academia Sinica, 230031-Hefei, People's Republic of China*

Y. Kawazoe

*Institute for Materials Research, Tohoku University, Sendai 980-8577, Japan*

(Received 6 July 1999; revised manuscript received 24 September 1999)

Complementary to our previous study [Wang *et al.*, Phys. Rev. B **59**, 12 672 (1999)], the intrinsic stability of the magic  $\text{Fe}_{13}\text{O}_8$  cluster is confirmed by the calculations on the vibrational properties. For all the vibration modes, the frequency is positive, and therefore the structure is dynamically stable.  $A_{1g}$ ,  $B_{1g}$ , and  $B_{2g}$  modes are Raman active,  $A_{2g}$ ,  $A_{2u}$ , and  $E_u$  modes are infrared active, while the  $E_g$  mode is active both in Raman and in infrared spectroscopy. The intrinsic stability combined with the relative stability make this cluster to be magic.

## I. INTRODUCTION

Transition-metal oxides show a rich variety of phenomena,<sup>1-3</sup> e.g., Mott transition, high- $T_c$  superconductivity, ferromagnetism, antiferromagnetism, low-spin to high-spin transitions, ferroelectricity, antiferroelectricity, colossal magnetoresistance, charge ordering, and bipolaron formation, which cover almost all the interesting phenomena in physics and in materials science. Therefore, extensive studies have already been devoted to this field. In recent years, with the new advent of flexible and precise experimental techniques, the studies on the oxidation of transition-metal clusters have also started to attract great attention: e.g.,  $\text{Fe}_n$ ,<sup>4-6</sup>  $\text{Cr}_n$ ,<sup>7</sup>  $\text{Mn}_n$ ,<sup>8,9</sup>  $\text{Co}_n$ ,<sup>10</sup> and  $\text{Nb}_n$  (Refs. 11 and 12) systems have already been studied. Among these systems, Fe-O clusters are of particular interest due to the diverse physical and chemical behaviors, and it is expected that well-controlled studies on iron oxide clusters will not only provide a new avenue to obtain detailed information about the interaction between oxygen and iron but also provide models for the iron oxide materials<sup>13</sup> and iron oxide surfaces.<sup>14,15</sup> Recently, a magic cluster  $\text{Fe}_{13}\text{O}_8$  has been found by using a reactive laser vaporized cluster source.<sup>16</sup> The equilibrium geometry, electronic structures, and magnetic properties are studied in detail in a previous work.<sup>17</sup> It has been found that this magic cluster has  $D_{4h}$  symmetry, in which there are three non-equivalent Fe atoms: the central Fe atom (labeled Fe1) and surface Fe2 and Fe3 atoms, as shown in Fig. 1. The bond

lengths and bond angles are as follows:  $r_{\text{O-Fe1}}=3.141 \text{ \AA}$ ,  $r_{\text{O-Fe2}}=1.848 \text{ \AA}$ ,  $r_{\text{O-Fe3}}=1.807 \text{ \AA}$ ,  $\angle \text{O-Fe2-O}=178.4^\circ$ , and  $\angle \text{O-Fe3-O}=159.1^\circ$ . The average binding energy per atom is 5.64 eV. Our central theoretical interest is the study

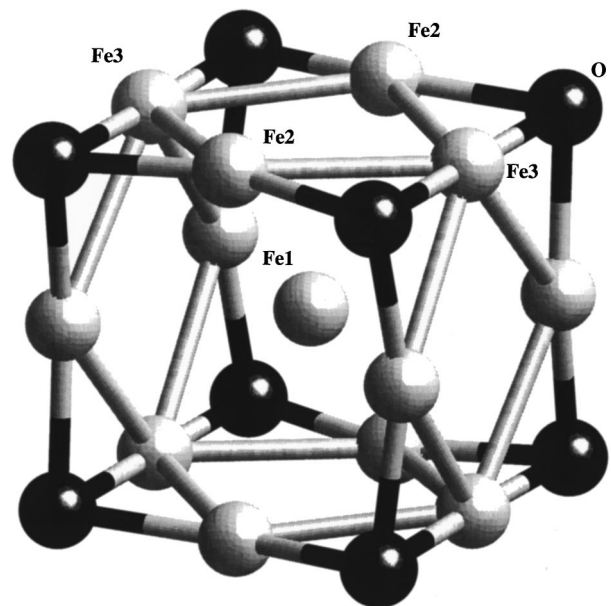


FIG. 1. The equilibrium structure of the  $\text{Fe}_{13}\text{O}_8$  magic cluster with  $D_{4h}$  symmetry.

TABLE I. Comparison of the bond length (in Å) and of the vibrational frequencies (in  $\text{cm}^{-1}$ ) obtained in the present calculation with the results of other calculations and experimental data for the  $\text{H}_2\text{O}$  molecule.

	Present cal.	All-electron cal. (Ref. 30)	Pseudopotential cal. (Ref. 30)	Expt. value (Ref. 31)
Bond length	0.975	0.970	1.125	0.960
Symmetric bending mode	1500	1547	1302	1595
Symmetric stretching mode	3795	3714	3010	3657
Asymmetric stretching mode	3915	3823	3018	3756

of stability of this magic cluster. The relative stability of  $\text{Fe}_{13}\text{O}_8$  has already been confirmed in our previous study<sup>17</sup> by comparing the binding energies and the gaps between the highest occupied molecular orbital (HOMO) and the lowest unoccupied molecular orbital (LUMO) for  $\text{Fe}_{13}\text{O}_6$ ,  $\text{Fe}_{12}\text{O}_9$ ,  $\text{Fe}_{14}\text{O}_7$ , and  $\text{Fe}_{13}\text{O}_8$  clusters. However, the intrinsic stability of this magic cluster has not, to the best of our knowledge, been studied yet. The *conventional* geometry optimizations converge to a structure on the potential energy surface where the force on the system is essentially zero and the structure may correspond to a minimum on the potential energy surface or it may represent a saddle point, which is a minimum with respect to some directions on the surface while a maximum in other direction(s). This ambiguity can be solved by analyzing the dynamical properties of the system. In fact, in the latter case, the system displays some imaginary frequencies, suggesting there are some geometry distortions for which the energy of the system is lower than it is in the current structure, such an instability in structure cannot be easily detected by a relative stability study. In this paper, we will calculate the vibrational eigenstates of the  $\text{Fe}_{13}\text{O}_8$  cluster to check its intrinsic stability; if all the vibration modes have positive frequency, the structure is dynamically stable, and the system has so-called intrinsic stability.

## II. THEORETICAL METHOD

The state-of-the art methods for calculating vibrational properties of crystals or clusters from first principles can be separated into two different categories: the linear-response method<sup>18–20</sup> and the direct (supercell) approach.<sup>21–25</sup> The modern implementation of the linear-response approach evaluates only the valence eigenfunctions and eigenvalues; the computational effort is equivalent or even less than for the direct method. In the direct method, the so-called frozen-phonon technique is used, where the phonon energy is calculated as a function of the displacement amplitude in terms of the energy difference between the distorted and the ideal lattice. This method is restricted to the systems whose vibrational wavelength is compatible with the size of unit cell. In the present calculation, we use the direct *ab initio* force constant approach employing a supercell with periodic boundary conditions.

Solving the dynamic equation

$$\mathbf{D} \cdot \mathbf{e} = \omega^2 \mathbf{e} \quad (1)$$

we obtain the vibration frequency  $\omega$  and eigenvectors  $\mathbf{e}$ , where the supercell dynamic matrix  $\mathbf{D}$  can be calculated

from the force constant matrix  $\Phi$  representing a bond between two atoms; the detailed formula can be found in Ref. 21.

The calculated frequency spectrum of the vibrational modes of the cluster can be efficiently displayed in terms of the partial density of states, describing the contribution to the density of state for the selected atom vibrating along a selected Cartesian coordinate, which is defined as

$$g_{i,\nu}(\omega) = \frac{1}{nd\Delta\omega} \sum_{\mathbf{K},j} |e_i(\mathbf{K},j;\nu)|^2 \delta_{\Delta\omega}(\omega - \omega(\mathbf{K},j)) \quad (2)$$

where  $e_i(\mathbf{K},j;\nu)$  is the  $i$ th Cartesian component of the eigenvector of the mode  $(\mathbf{K},j)$  for the  $\nu$  atom,  $\Delta\omega$  is the broadening factor,  $n$  is the number of sampling wave-vector points,  $d$  is the dimension of the dynamic matrix, and  $\delta_{\Delta\omega}(x)$  equals 1 if  $|x| \leq \Delta\omega/2$ , otherwise it is zero.

The total vibrational density of states can be obtained

$$g(\omega) = \sum_{i,\nu} g_{i,\nu}(\omega) \quad (3)$$

where summation  $\nu$  runs over the atom and  $i$  runs over the Cartesian component.

## III. RESULTS AND DISCUSSION

In the present calculations, the Hellmann-Feynman forces are obtained using the *ab initio* plane-wave ultrasoft pseudopotential scheme Vienna *Ab initio* Simulation Program (VASP),<sup>26–28</sup> further details of the calculation can be found in Ref. 17. To solve the eigenvalue problem for the dynamic matrix Eq. (1), we used the method described in Ref. 21, as implemented in the PHONON program.<sup>29</sup> In order to test our calculations, first we performed calculations on the  $\text{H}_2\text{O}$  molecule by putting this molecule in the supercell with  $8 \times 9 \times 10 \text{ \AA}^3$ . The results are shown in Table I. The comparison with the experimental values is reasonable.

For the  $\text{Fe}_{13}\text{O}_8$  cluster, the supercell is  $12.5 \times 12.5 \times 13.4 \text{ \AA}^3$ , which is sufficiently large to make dispersion effects negligible. A kinetic-energy cutoff of 430 eV has been used in the plane-wave expansion of the pseudowave functions, which is large enough to obtain a good convergence (the changes of the total energy are of the order of only 0.7 meV if the kinetic-energy cutoff is increased to 450 eV). For the exchange-correlation energy of valence electrons, we adopted the form of Ceperley and Alder<sup>32</sup> as parametrized by Perdew and Zunger.<sup>33</sup>

For the amplitude of displacement, we have made exten-

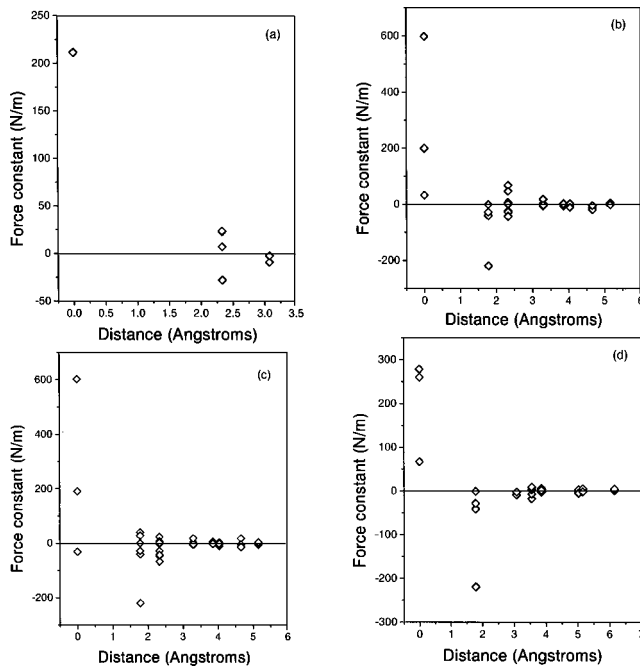


FIG. 2. Force constants as a function of distance for the Fe1 (a), Fe2 (b), Fe3 (c), and O atoms (d).

sive tests. Much attention should be paid to preserve the linearity of the force as a function of displacement amplitude; too large a displacement will destroy the linearity, while too small a displacement will cause too much calculation noise. Taking into account the symmetry of the cluster, the Hellman-Feynman forces are computed for ten independent configurations: two with the Fe1 atom displaced along the  $x$  and  $z$  direction at an amount of 0.025 and 0.027 Å, respectively, to preserve linearity; three with the Fe2 atom displaced along  $x$  (0.031 Å),  $y$  (0.013 Å), and  $z$  (0.033 Å); three with the Fe3 atom displaced along  $x$  (0.031 Å),  $y$  (0.031 Å), and  $z$  (0.013 Å); two with the O atom displaced along  $x$  (0.025 Å), and  $z$  (0.027 Å). Each displacement generates  $3 \times 21 = 63$  force components. Therefore, the ten chosen independent configurations in total produce 630 data of Hellmann-Feynman forces. Fitting these data gives 154 independent parameters for force constants. Figures 2(a)–2(d) show the force constant changes with the distance for the Fe1, Fe2, Fe3, and O atoms, respectively. It can be found that the force constant rapidly decreases with distance, suggesting that our supercell is large enough to obtain the vibrating properties with an appreciable accuracy.

With the broadening factor of 0.1 THz, Figs. 3–6 show the partial density of states obtained for vibration along the independent directions for the Fe1, Fe2, Fe3, and O atoms, respectively. Figure 7 shows the total density of states for the cluster. From our results we obtained the following conclusions.

(i) The frequencies for all the vibration modes are positive. Therefore, the structure is dynamically stable, and the Fe<sub>13</sub>O<sub>8</sub> cluster has intrinsic stability. The intrinsic stability together with the relative stability make this cluster to be magic, resulting in a very sharp peak in the time-of-flight mass spectra.<sup>16,17</sup>

(ii) Because the nearest-neighbor distance for the Fe1

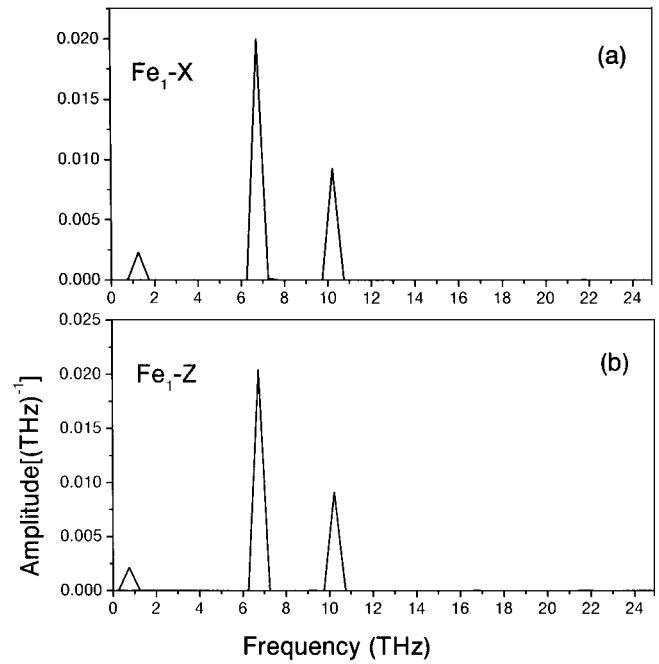


FIG. 3. Partial density of states for the Fe1 atom vibrating along the  $x$  direction (a) and  $z$  direction (b). The vibration along the  $y$  direction is equivalent to that in the  $x$  direction.

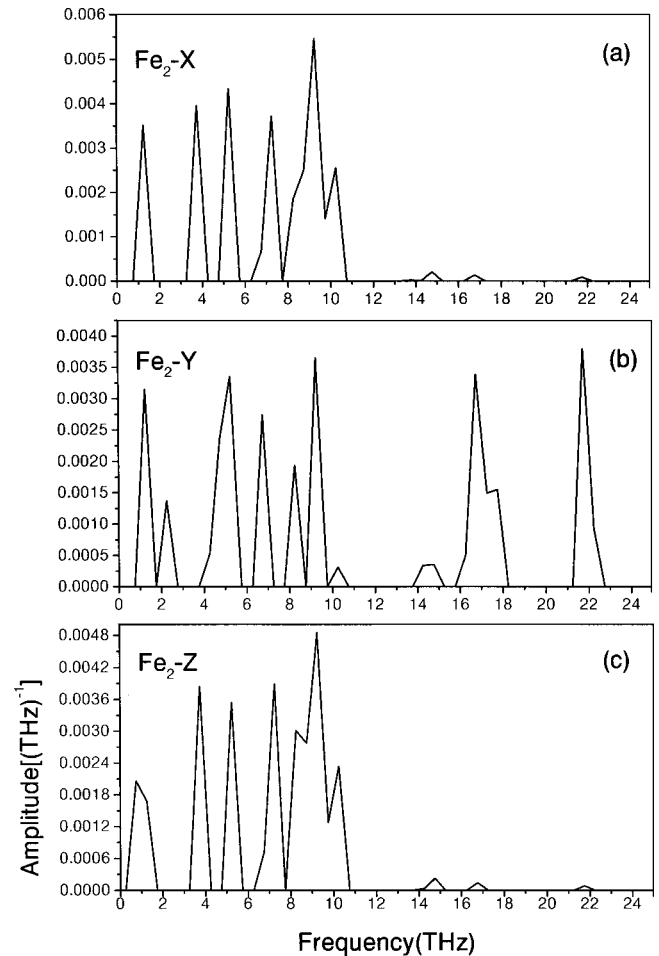


FIG. 4. Partial density of states for the Fe2 atom vibrating along the  $x$  direction (a),  $y$  direction (b), and  $z$  direction (c).

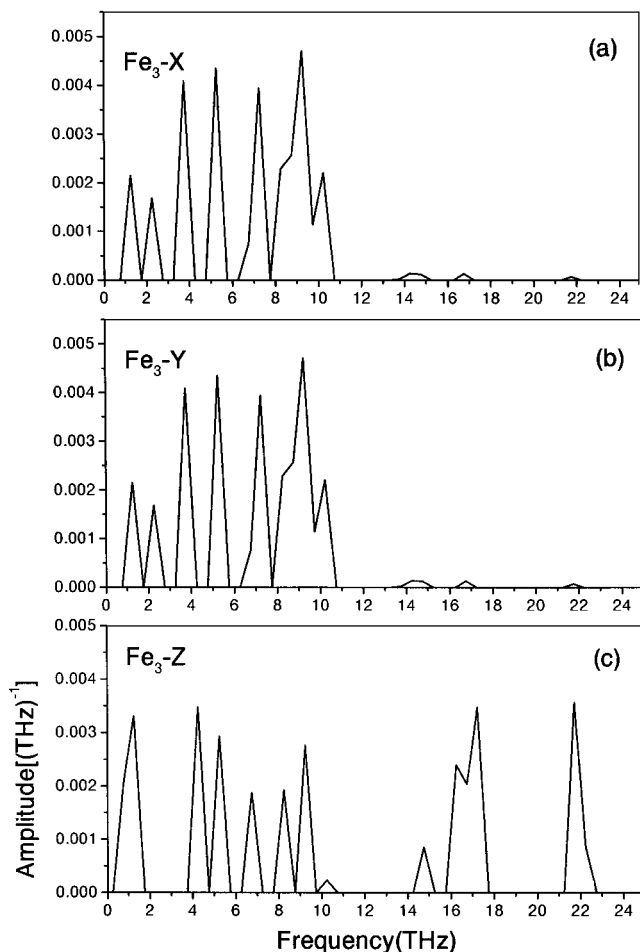


FIG. 5. Partial density of states for the Fe3 atom vibrating along the  $x$  direction (a),  $y$  direction (b), and  $z$  direction (c).

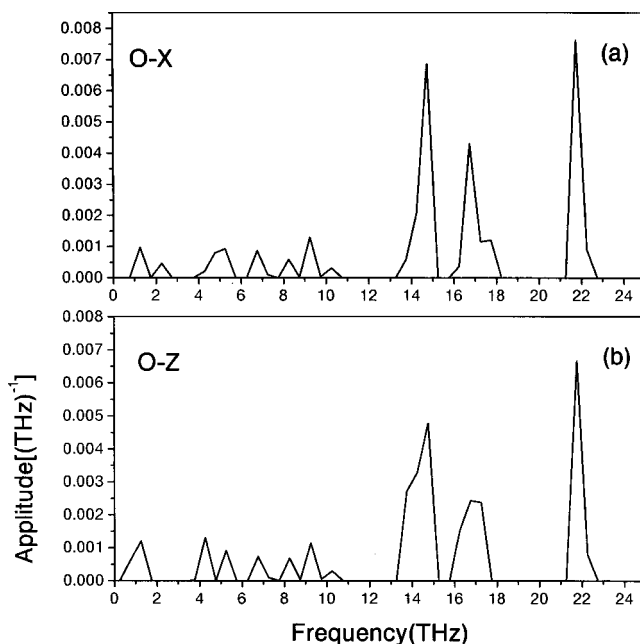


FIG. 6. Partial density of states for the O atom vibrating along the  $x$  direction (a) and  $z$  direction (b). The vibration along the  $y$  direction is equivalent to that in the  $x$  direction.

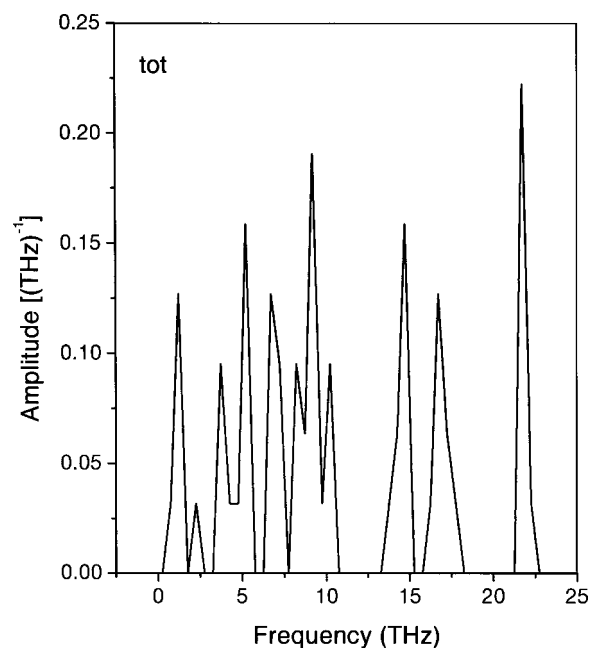


FIG. 7. Total vibrational density of states for the  $\text{Fe}_{13}\text{O}_8$  cluster.

atom is 2.430 Å, larger than those of the Fe2 (1.848 Å) and Fe3 (1.807 Å) atoms, the interaction between the Fe1 atom and its nearest neighbors is weaker than for the other iron atoms. Accordingly, the vibrational frequencies of the modes in which mainly the Fe1 atom moves are lower than those of the modes more or less localized on the other iron atoms. The Fe2 atom vibrates with high frequency in the  $y$  direction, while the Fe3 one shows its high frequency regime for vibration in the  $z$  direction.

(iii) Compared to the Fe atom, the O atom is much lighter in mass; as a result, the vibrating frequency of the O atom is much larger than that of the Fe atom.

(iv) It is possible to probe the vibrational properties of a cluster by infrared (IR) and Raman (R) techniques to obtain the structural information of a cluster, as it has already been applied to the  $\text{C}_{60}$  dimer.<sup>34</sup> For future comparison with experiment, Table II shows the vibration modes active in Raman (R) or/and infrared (IR) spectroscopy, the corresponding irreducible representations (IrRep) are also given.  $A_{1g}$ ,  $B_{1g}$ , and  $B_{2g}$  modes are Raman active,  $A_{2g}$ ,  $A_{2u}$ , and  $E_u$  modes are infrared active, while the  $E_g$  mode is active in Raman as well as in infrared spectroscopy.

TABLE II. Frequencies (in  $\text{cm}^{-1}$ ) and irreducible representations of the vibrational modes active in Raman or/and infrared spectroscopy for the  $\text{Fe}_{13}\text{O}_8$  cluster.

	IrRep	Frequency
R	$A_{1g}$	5.44, 8.88, 9.89, 14.11, 22.16
	$B_{1g}$	5.21, 8.82, 14.62
	$B_{2g}$	4.89, 9.15, 14.24, 21.74
IR	$A_{2g}$	8.25, 17.84
	$A_{1u}$	6.63, 9.35, 10.15, 17.26
	$E_u$	3.90, 6.67, 7.02, 9.28, 14.86, 17.28, 22.12
R+IR	$E_g$	5.25, 8.26, 15.10, 17.22, 21.69

In summary, by using an approach based on the first-principles force constant method, the intrinsic stability of the  $\text{Fe}_{13}\text{O}_8$  cluster has been investigated and confirmed. Furthermore, it has been pointed out that this study can be relevant as a supplementary tool to the usual static minimization procedure.<sup>17</sup>

#### ACKNOWLEDGMENT

The authors would like to express their sincere thanks to the Materials Information Science Group of the Institute for Materials Research, Tohoku University, for its continuous support of the HITAC S-3800/380 supercomputing facility.

- 
- <sup>1</sup>C.N.R. Rao and B. Raveau, *Transition Metal Oxides* (Wiley-vch, New York, 1998).
- <sup>2</sup>V.E. Henrich and P.A. Cox, *The Surface Science of Metal Oxides* (Cambridge University Press, Cambridge, England, 1994).
- <sup>3</sup>P.A. Cox, *Transition Metal Oxides* (Clarendon Press, Oxford, 1992).
- <sup>4</sup>L.S. Wang, H.B. Wu, and S.R. Desai, *Phys. Rev. Lett.* **76**, 4853 (1996).
- <sup>5</sup>L.S. Wang, J.W. Fan, and L. Lou, *Surf. Rev. Lett.* **3**, 695 (1996).
- <sup>6</sup>H.B. Wu, S.R. Desai, and L.S. Wang, *J. Am. Chem. Soc.* **118**, 5296 (1996).
- <sup>7</sup>S. Veliah, K.H. Xiang, R. Pandey, J.M. Recio, and J.M. Newsam, *J. Phys. Chem. B* **102**, 1126 (1998).
- <sup>8</sup>P.J. Ziemann and A.W. Castlemann, Jr., *J. Chem. Phys.* **94**, 718 (1991).
- <sup>9</sup>S.K. Nayak and P. Jena, *Phys. Rev. Lett.* **81**, 2970 (1998).
- <sup>10</sup>M.P. Robben, P.H. Rieger, and W.E. Geiger, *J. Am. Chem. Soc.* **121**, 367 (1999).
- <sup>11</sup>J. Mwakapumba and K.N. Ervin, *Int. J. Mass Spectrom. Ion Processes* **161**, 161 (1997).
- <sup>12</sup>H.G. Gronbeck, A. Rosen, and W. Andreoni, *Z. Phys. D: At., Mol. Clusters* **40**, 206 (1997).
- <sup>13</sup>J.S. Corneille, J.W. He, and D.W. Goodman, *Surf. Sci.* **338**, 211 (1995).
- <sup>14</sup>N.G. Conden, *Phys. Rev. Lett.* **75**, 1961 (1995).
- <sup>15</sup>R. Wiesendanger, *Science* **255**, 583 (1992).
- <sup>16</sup>M. Sakurai, K. Sumiyama, Q. Sun, and Y. Kawazoe, *J. Phys. Soc. Jpn.* **68**, 3497 (1999).
- <sup>17</sup>Q. Wang, Q. Sun, M. Sakurai, Z.J. Yu, B.L. Gu, K. Sumiyama, and Y. Kawazoe, *Phys. Rev. B* **59**, 12 672 (1999).
- <sup>18</sup>R.D. King-Smith and R.J. Needs, *J. Phys.: Condens. Matter* **2**, 3431 (1990).
- <sup>19</sup>P. Giannozzi, S. de Gironcoli, P. Pavone, and S. Baroni, *Phys. Rev. B* **43**, 7231 (1991).
- <sup>20</sup>O. Schütt, P. Pavone, W. Windl, K. Karch, and D. Strauch, *Phys. Rev. B* **50**, 17 054 (1994).
- <sup>21</sup>K. Parlinski, Z.Q. Li, and Y. Kawazoe, *Phys. Rev. Lett.* **78**, 4063 (1997).
- <sup>22</sup>K. Parlinski and Y. Kawazoe, *Phase Transit.* **65**, 73 (1998).
- <sup>23</sup>K. Kunc and R.M. Martin, *Phys. Rev. Lett.* **48**, 406 (1982).
- <sup>24</sup>S. Wei and R.M. Chou, *Phys. Rev. Lett.* **69**, 2799 (1992).
- <sup>25</sup>W. Franck, C. Elsässer, and M. Fähnle, *Phys. Rev. Lett.* **74**, 1791 (1995).
- <sup>26</sup>G. Kresse and J. Hafner, *Phys. Rev. B* **47**, 558 (1993); **49**, 14 251 (1994).
- <sup>27</sup>G. Kresse and J. Furthmüller, *Phys. Rev. B* **54**, 11 169 (1996).
- <sup>28</sup>G. Kresse and J. Hafner, *J. Phys.: Condens. Matter* **6**, 8245 (1994).
- <sup>29</sup>K. Parlinski, *Software Phonon*, 1999.
- <sup>30</sup>A. Briley, M.R. Pederson, K.A. Jackson, and D. V. Porezag, *Phys. Rev. B* **58**, 1786 (1998).
- <sup>31</sup>H. Haken and H.C. Wolf, *Molecular Physics and Elements of Quantum Chemistry* (Springer-Verlag, Berlin, 1995).
- <sup>32</sup>D.M. Ceperley and B.J. Alder, *Phys. Rev. Lett.* **4**, 566 (1980).
- <sup>33</sup>J.P. Perdew and A. Zunger, *Phys. Rev. B* **23**, 5048 (1981).
- <sup>34</sup>J. Onoe and K. Takeuchi, *Phys. Rev. B* **54**, 6167 (1996).